Dynamic Response of Lift Systems Under Overtravel and Buffer Impact Conditions

Stefan Kaczmarczyk

School of Technology, Faculty of Education, Arts, Science and Technology
University of Northampton

Keywords: Overtravel, Buffer, Gravity Stopping Distance, Dynamic Responses, Acceleration.

Abstract. The overtravel arrest mechanism consists of buffers beneath the car and often beneath the counterweight. During lift car/counterweight buffering, both in free fall and in the scenario when the suspension remains intact, various adverse dynamic phenomena may occur and should be considered. This paper presents simplified models for predicting the dynamic behaviour of a lift system during overtravel under buffer-strike conditions. The models incorporate both linear and nonlinear buffer characteristics and are implemented in a computer simulation environment. Simulation tests are conducted over a range of buffer impact speeds and lift system parameters to evaluate buffering forces and impact-induced dynamic phenomena.

1 INTRODUCTION

There are a range of circumstances where an emergency arrest must be initiated during operation of a lift system. These include overtravel of terminal floors, either at the top or bottom of the hoistway. This may result from several factors, including failure of brake components, reduced brake friction, or the brake failing to release when de-energised; as well as traction machine failure, loss of traction, or control system malfunction.

BS EN 81-20 [1] requires lift installations to be fitted with buffers beneath both the car and the counterweight, providing a means of emergency arrest in the event of overtravel beyond the designated terminal floor. Three types of buffer are permitted: linear energy accumulation buffers, non-linear energy-accumulation buffers, and energy dissipation buffers.

Linear energy accumulation buffers consist of mechanical springs with linear characteristics, while the non-linear type consists of blocks made of polyurethane material (foam). The impact energy is stored in the form of elastic strain energy. The use of accumulation buffers is restricted to rated speeds up to 1 m/s.

For higher rated speeds, codes require that buffers dissipate the impact energy during the stopping stroke, i.e., as the buffer is compressed, so that no rebound of the car/counterweight occurs. In this case, the impact energy is dissipated rather than stored. This requirement is met by energy dissipation buffers, which are typically hydraulic (oil) in type. Such buffers can be used for lifts of all rated speeds.

2 THE DYNAMIC BEHAVIOUR

2.1 Dynamic model

Figure 1(a) shows a simplified model of a lift under buffering at the car side. Here M_1, M_2 and M_{sr} denote the masses of the car, counterweight and suspension ropes, respectively, while x_1, x_2, v_1, v_2 and a_1, a_2 represent their respective displacements, velocities, and accelerations. The diagram illustrates the car impacting the buffer, where F_b represents the buffering force. This model is subsequently used to analyse the lift dynamics and impact-induced phenomena.

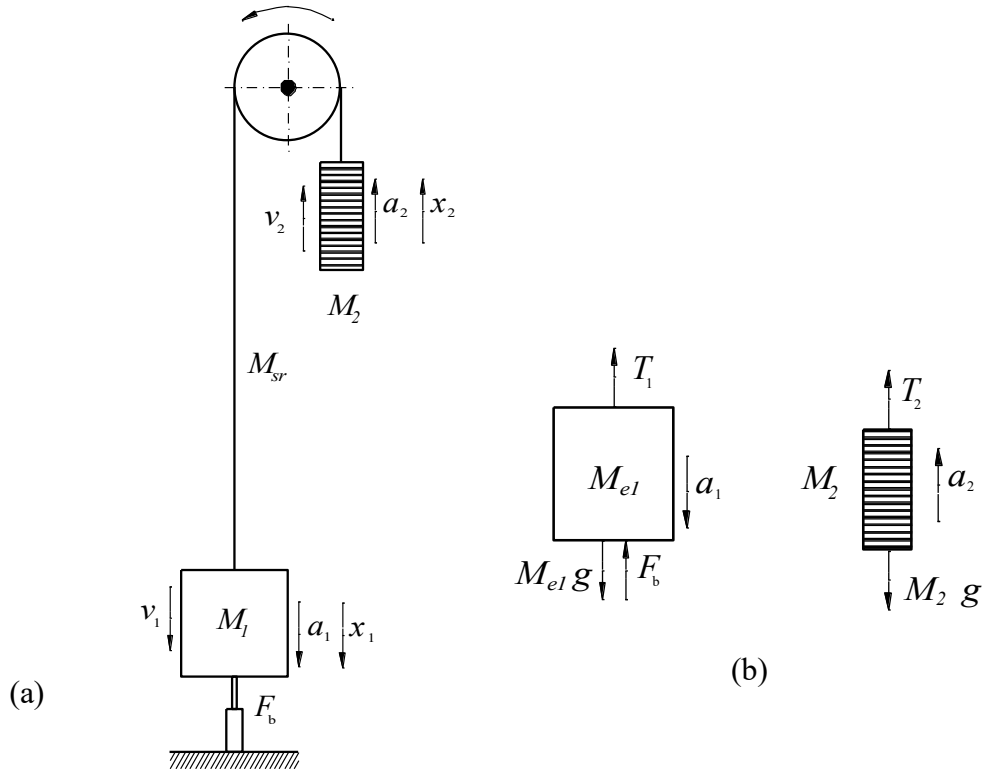


Figure 1 Lift system under buffering

Figure 1(b) shows free-body diagrams identifying the forces acting at the car and counterweight sides, respectively. Here $M_{e1} = M_1 + M_{sr}$ represents the equivalent well masses at the car side, which include the mass of suspension ropes. The mass of the short length of suspension ropes at the counterweight side is neglected in the analysis. Using Newton's second law, the balance of forces at the car and counterweight sides is given as

$$M_{e1}\ddot{x}_1 = M_{e1}g - T_1 - F_b \quad (1)$$

$$M_2\ddot{x}_2 = T_2 - M_2 g \quad (2)$$

where over dots denote the second time derivatives so that $\ddot{x}_1 = a_1$ and $\ddot{x}_2 = a_2$, T_1, T_2 represent the rope tensions at the car and counterweight sides, respectively, and g is the acceleration of gravity. Friction forces are much smaller than the buffering forces involved and are neglected in the model. Flexibility of suspension ropes is also neglected in the model given by Equations 1 - 2.

Consider a scenario when the traction drive/machine has failed, and the electromechanical brake has not engaged, resulting in a buffering event. For a low inertia machine such as a gearless lift system, the inertia of the traction machine/sheave can be neglected during the buffering stop [2], and $T_1 = T_2 = T$, $x_1 = x_2 = x$ can be used in (1) and (2). With intact suspension, the car and counterweight remain coupled (by taught ropes) when the system deceleration is no more than 1g. The motion of the coupled system is then governed by the following equation

$$M_{eff}\ddot{x} + F_b = F_0 \quad (3)$$

where $M_{eff} = M_{e1} + M_2$ represents the effective mass of the coupled system, and $F_0 = (M_{e1} - M_2)g$.

If the deceleration is greater than 1g, the suspension ropes become slack ($T = 0$), and the equations of motion of the uncoupled system are

$$\ddot{x}_1 = g - \frac{F_b}{M_{e1}} \tag{4}$$

$$\ddot{x}_2 = -g \tag{5}$$

Equation 4 describes the motion of the car, while Equation 5 defines the motion of the counterweight, which decelerates under gravity. As it descends, the counterweight may re-engage with the suspension, causing the ropes to become taut again. During such an event, referred to as a "counterweight jump", the potential for impact loading on the ropes should be assessed [3].

2.2 Energy accumulation buffers

2.2.1 Linear spring buffers

When a linear spring buffer is compressed by a descending car, the kinetic and potential energy of the net descending mass is 'accumulated' in the compressed spring and will cause a rebound once the descending mass has been arrested. Therefore, the use of linear spring buffers is limited to low-speed installations.

EN81 stipulates that the total possible stroke of the buffers shall be at least equal to twice the gravity stopping distance corresponding to 115% of the rated speed. The minimum stroke is therefore determined as

$$s_{acc} = \frac{(1.15v)^2}{g} \tag{6}$$

In addition, it should be designed that a static load of between 2.5 and 4 times the sum of the mass of the car and its rated load should produce the stroke. This requirement is expressed by

$$(2.5 \div 4)\frac{(P+Q)g}{k} = s_{acc} \tag{7}$$

where P denotes the car mass, Q is the rated load, and k represents the spring constant. Equation 7 defines the range of spring stiffness allowed in EN81. The corresponding buffering forces in Equations 3 and 4 for the coupled system ($T > 0$) and the uncoupled car ($T = 0$) are then defined as

$$F_b = \begin{cases} kx, & T > 0 \\ kx_1, & T = 0 \end{cases} \tag{8}$$

respectively. The dynamic response of the coupled system defined by Equation 3 is then expressed as

$$\ddot{x} + \omega_n^2 x = f_0 \tag{9}$$

where $\omega_n = \sqrt{\frac{k}{M_{eff}}}$ and $f_0 = \frac{F_0}{M_{eff}}$. Once tension in the suspension is lost, Equation 4 describing the uncoupled response of the car is expressed as

$$\ddot{x}_1 + \omega_{1n}^2 x_1 = g \tag{10}$$

where $\omega_{1n} = \sqrt{\frac{k}{M_{e1}}}$. The counterweight ascending/descending motions are determined by Equation 5. Equations 5, 9 and 10 are linear and, with the corresponding initial conditions, can be solved analytically.

The solution of Equation 9 is defined as follows.

$$\begin{aligned} x(t) &= \frac{F_0}{k} + \left(x_0 - \frac{F_0}{k} \right) \cos \omega_n t + \frac{\dot{x}_0}{\omega_n} \sin \omega_n t \\ \dot{x}(t) &= \dot{x}_0 \cos \omega_n t - \left(x_0 - \frac{F_0}{k} \right) \omega_n \sin \omega_n t \end{aligned} \tag{11}$$

The above solution is defined over the time interval $0 \le t \le t_{f1}$, where t_{f1} denotes the time instant when tension in the suspension is lost. Considering that the initial time $t = 0$ represents the instant of the impact and the buffer is not deflected yet, the initial conditions are assumed as

$$x_0 = x(0) = 0,\ \dot{x}_0 = \dot{x}(0) = 1.15v \tag{12}$$

The solution of the equation defining the uncoupled motion of the car (10) is given as

$$\begin{aligned} x_1(t) &= \frac{M_{e1} g}{k} + \left(x_{10} - \frac{M_{e1} g}{k} \right) \cos \omega_{1n} \left(t - t_{f1} \right) + \frac{\dot{x}_{10}}{\omega_{1n}} \sin \omega_{1n} \left(t - t_{f1} \right) \\ \dot{x}_1(t) &= \dot{x}_{10} \cos \omega_{1n} \left(t - t_{f1} \right) - \left(x_{10} - \frac{M_{e1} g}{k} \right) \omega_{1n} \sin \omega_{1n} \left(t - t_{f1} \right) \end{aligned} \tag{13}$$

This solution is valid for the time interval $t_{f1} \le t \le t_f$, where t_f is the time instant when the suspension becomes tensioned again. The initial conditions that apply here are defined as $x_{10} = x\left(t_{f1}\right)$, $\dot{x}_{10} = \dot{x}\left(t_{f1}\right)$, respectively. On the other hand, the solution of Equation 5 over the time interval $t_{f1} \le t \le t_f$, defining the uncoupled motion of the counterweight, is determined as

$$\begin{aligned} x_2(t) &= x\left(t_{f1}\right) - \dot{x}\left(t_{f1}\right) t_{f1} - \frac{1}{2} g t_{f1}^2 + \left[\dot{x}\left(t_{f1}\right) + g t_{f1} \right] t - \frac{1}{2} g t^2 \\ \dot{x}_2(t) &= \dot{x}\left(t_{f1}\right) + g t_{f1} - g t \end{aligned} \tag{14}$$

where the initial conditions $x_{20} = x\left(t_{f1}\right)$, $\dot{x}_{20} = \dot{x}\left(t_{f1}\right)$ are applied. The condition for the suspension to become taut again can then be defined as

$$x_1\left(t_f\right) = x_2\left(t_f\right) \tag{15}$$

2.2.2 Non-linear buffers

Energy accumulation buffers with non-linear characteristics are required to be type-tested. EN81-20 specifies that the deceleration of a free-falling car with its rated load evaluated in accordance with EN81-50 [4] should not be more than 1g. The method of evaluation is outlined in clause 5.5.3.2.6.1 a) of EN81-50, where it is specified that the deceleration should be determined considering the time between the first two absolute minima. EN81-20 also stipulates that the deceleration peaks of more than 2.5 g should not be longer than 0.04 s (40 ms), and the maximum peak is to be limited to 6 g.

A typical force-deflection characteristic curve of a nonlinear buffer is shown in Figure 2. The curve displays non-linear and hysteretic behaviour typical for polyurethane (PU) foam materials under loading (compressing) and unloading conditions. It consists of three distinct regions: linear elastic, plateau, and steep rise. During unloading, the force is much lower in comparison with the loading (compression) phase. The hysteresis loop illustrates the capacity to absorb/dissipate energy by the buffer. The area under the loading curve represents the total energy/work input, while the area under the unloading curve represents the returned energy. The area between the two curves is the absorbed/dissipated energy by the buffer.

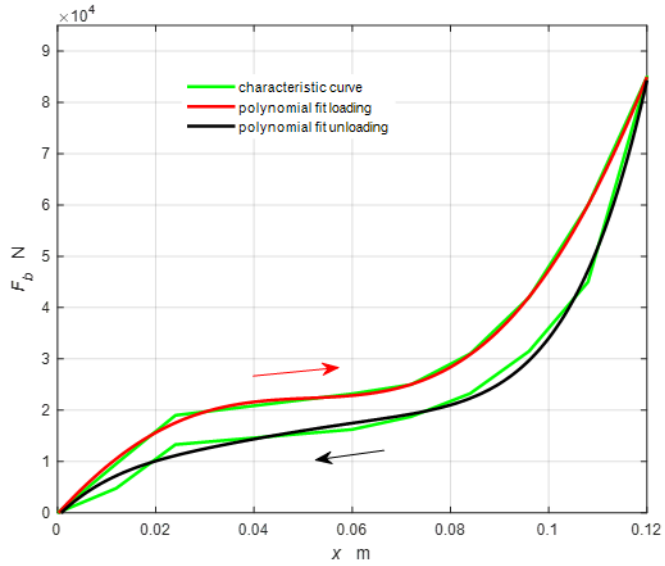


Figure 2 Non-linear buffer characteristic curve

A 5th-order polynomial can be applied to approximate the buffering force–deflection characteristic of the nonlinear buffer. The polynomial approximation is expressed by

$$F_b(x) = p_1x^5 + p_2x^4 + p_3x^3 + p_4x^2 + p_5x + p_6 \tag{16}$$

Equations 3-4 become nonlinear then, and a closed-form analytical solution cannot be readily developed. However, the system of nonlinear Equations 3-4 together with Equation 5 can be solved numerically.

2.3 Dissipation buffers

The application of energy accumulation type buffers, whether linear or non-linear, is generally limited to rated speeds below 1.0 m/s. Under some codes, the application is extended to higher speeds if there is a means of damping or 'buffering' the return movement as the car (or counterweight) rebounds from the maximum dynamic deflection [3].

At higher speeds, codes demand that the buffer should dissipate the kinetic energy during the stopping stroke, i.e. as the buffer is depressed, so that there is no rebound of the car/counterweight. This is achieved using a hydraulic buffer system.

EN81 stipulates that an energy dissipation (hydraulic) buffer is required to arrest the mass of the car with its rated load impacting the buffer in free fall with a speed of 115% of the rated speed at the average deceleration not greater than 1g. The minimum stroke for an energy dissipation type buffer is the gravity stopping distance corresponding to 115% rated speed. In a similar fashion to nonlinear energy accumulation buffers, the deceleration peaks of more than 2.5g should not be longer than 0.04 s.

There are various designs of hydraulic buffers [5]. In principle, the designs comprise a piston driven by the descending car (or counterweight) into a hydraulic fluid (oil). The fluid is then being transferred through restricting holes (orifices/throttles). The flow rate is a function of the orifice area [6] and is given by

$$q = C_d A_o \sqrt{\frac{2\Delta p}{\rho}} \tag{17}$$

where C_d is the coefficient of discharge, A_o denotes the orifice area, ρ represents the fluid mass density, and Δp is the pressure drop across the orifice. On the other hand, neglecting the fluid compressibility, continuity of the flow requires that

$$q = A_p v \tag{18}$$

where A_p is the piston area, and v is the speed of the piston. The pressure drop therefore is determined from Equations 17 and 18 as

$$\Delta p = \frac{\rho}{2}\left(\frac{A_p}{C_d A_o}\right)^2 v^2 \tag{19}$$

The buffering force developed due to the restriction of the hydraulic flow is determined as

$$F_{bh} = A_p \Delta p = A_p \frac{\rho}{2}\left(\frac{A_p}{C_d A_o}\right)^2 v^2 \tag{20}$$

In hydraulic buffer systems, the effective orifice flow area is not constant but varies with piston displacement due to progressive restriction of flow passages (e.g., covering of orifices or metering geometries), resulting in a nonlinear force–stroke characteristic.

With the orifice area defined as $A_o = A_o(x)$, the hydraulic buffering force is expressed as

$$F_{bh}(x,\dot{x}) = c_b(x)\dot{x}^2 \tag{21}$$

where

$$c_b(x) = A_p \frac{\rho}{2}\left(\frac{A_p}{C_d A_o(x)}\right)^2 \tag{22}$$

The buffer design includes a return spring (mechanical or gas spring). The return spring will accumulate a small fraction of the total energy to be dissipated during the buffering event. The accumulated energy is then used to return the piston to its normal extended position after the buffering operation. If the return spring's constant is denoted by *k,* the total force acting upon the car is given as

$$F_b(x,\dot{x}) = c_b(x)\dot{x}^2 + kx \tag{23}$$

The equation of motion (3) assumes the following form then

$$M_{eff}\ddot{x} + c_b(x)\dot{x}^2 + kx = F_0 \tag{24}$$

3 CASE STUDY AND EXAMPLES

In this section, the dynamic behaviour of a lift system under buffer-strike conditions is demonstrated by applying the models developed in the preceding section. Consider a lift system of rated load Q = 800 kg, comprising a car of estimated mass P = 960 kg. The travel height is H = 25 m and the counterweight is balanced at 50%. A suspension comprising four 13 mm steel wire ropes (SWR) with fibre core (FC) of mass per unit length 0.569 kg/m each is used in the installation. In the examples below, these parameters are applied to demonstrate the performance of the energy accumulation and energy dissipation buffers.

3.1 Performance example of energy accumulation buffers

3.1.1 Linear spring buffer

The analytical solutions of Equations 9-10 are defined by Equations 11 and 10, respectively. In addition, Equations 14 and 15 define the solution of Equation 5. These are applied to carry out calculations defining the buffer performance. The diagrams shown in Figure 3 illustrate the performance of a linear spring buffer for a fully loaded car of rated speed 1 m/s with suspension intact. Using Equation 6, the minimum stroke is determined as $s_{acc} = 0.1348$ m and the stiffness of the spring is selected as $k = 2.5\dfrac{(P+Q)g}{s_{acc}} = 3.2018\times10^{5}$ N/m.

The diagram in Figure 3(a) shows the displacements of the system evaluated from the instant of the car impact. The car and counterweight remain coupled until the time instant is approx. 0.11 s, when the deceleration reaches 1g (see the diagram in Figure 3(c)) and the ropes become slack. The counterweight continues its ascent, decelerating under gravity while the car is descending and then ascending on the buffer. The ascending counterweight comes to rest momentarily at the time instant of about 0.175 s and then drops back, re-engaging with the suspension at the time instant of about 0.331 s (see the area encircled in green). The speed of the counterweight when it drops back onto the suspension is 1.52 m/s as determined from the velocity diagram in Figure 3(b) (see the area encircled in green). This may impose a significant impact loading on the suspension ropes.

The car acceleration curve plotted in Figure 3(c) demonstrates that in approximately the middle of the buffering event, the deceleration exceeds 1g (however, the mean/average deceleration is less than 1g). As expected, in the region where the car deceleration is over 1g, the corresponding buffering forces reach their maximum values.

Equation 10 describing uncoupled motion of the car and its solution given by Equation 13 can also be used to predict buffering of the car in free fall. The initial conditions are then in line with Equation 12 written in the form

$$x_{10} = x_1(0) = 0,\ \dot{x}_{10} = \dot{x}_{10}(0) = 1.15v \tag{25}$$

The solution is then defined over the time interval $0 \le t \le t_f$, so that $t_{f1} = 0$ must be substituted into Equation 13. Figure 4 illustrates the evolution of displacement, velocity, acceleration, and buffering force over this interval, with $t_f = 0.3$ s, a motion cycle like that of the intact suspension system. It is evident that the displacement, velocity, acceleration, and buffering force are all greater than those observed in the intact suspension case.

3.1.1 Non-linear buffer

The buffer characteristic presented in Figure 2 is applied in the simulation. The following coefficients are used in Equation 16 to generate the loading/unloading polynomial fits:

$$\mathbf{p}_{loading} = \begin{bmatrix} -9.789325 & 2.95647 & -0.14916 & -0.01051 & 0.00104 & -0.00000022 \end{bmatrix} \times 10^{9}$$
$$\mathbf{p}_{unloading} = \begin{bmatrix} 2.926493 & -0.68354 & 0.06394 & -0.00309 & 0.00009 & -0.00000007 \end{bmatrix} \times 10^{10} \quad (26)$$

The nonlinear characteristics based on coefficients in Equation 26 are then applied in a numerical solution of Equation 3. Figure 5 shows plots that demonstrate the performance of the non-linear buffer for a fully loaded car of rated speed 1 m/s with intact suspension. The car and counterweight remain coupled until a time instant of approx. 0.093 s, when the deceleration reaches 1g (as can be seen from the deceleration plot in the diagram in Figure 5(c)) and the ropes become slack. Like in the case of the linear buffer, the counterweight continues its ascent, decelerating under gravity while the car is descending and then ascending on the buffer.

The ascending counterweight comes to rest momentarily at the time instant of about 0.16 s and then drops back, re-engaging with the suspension at the time instant of about 0.286 s (see the area encircled in green). The speed of the counterweight when it drops back onto the suspension is 1.23 m/s as determined from the velocity diagram in Figure 5(b) (see the area encircled in green). The effects of the buffer hysteretic behaviour on the car deceleration can be observed in the acceleration and buffering force plots presented in Figure 5(c). The unloading phase commences after the uncoupled car displacement reaches its maximum (after the time instant of approx. 0.134 s). The buffering force then drops abruptly to a lower value (see the force vs displacement plot in Figure 7), resulting in a sudden increase in the car's deceleration.

The evolution of displacements, velocity, acceleration and buffering forces for the car in free fall is illustrated by the plots in Figure 6, and Figure 8 shows the corresponding buffering force vs displacement plot. It is evident that the car decelerations are much higher than those with suspension intact. The peak deceleration at the time instant of about 0.12 s exceeds 2.5g. However, it can be detected that the values last no longer than 40 ms.

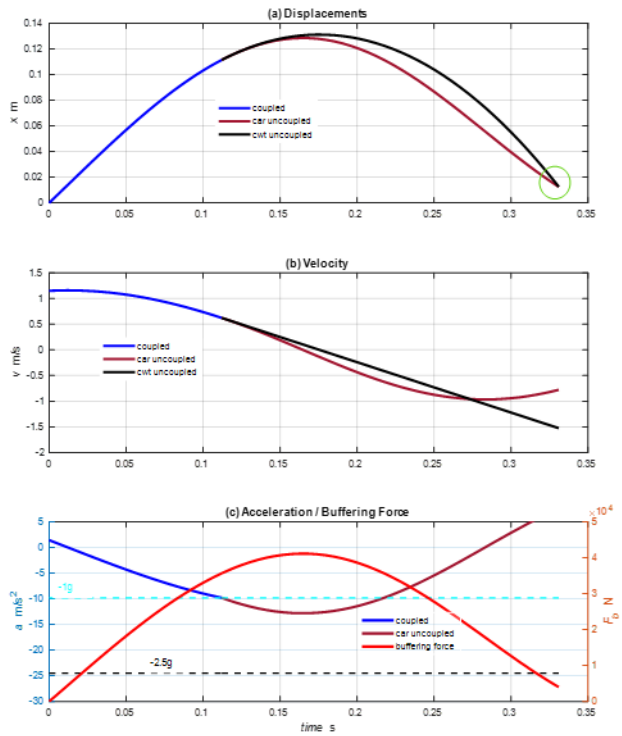


Figure 3 Linear spring accumulation buffer performance

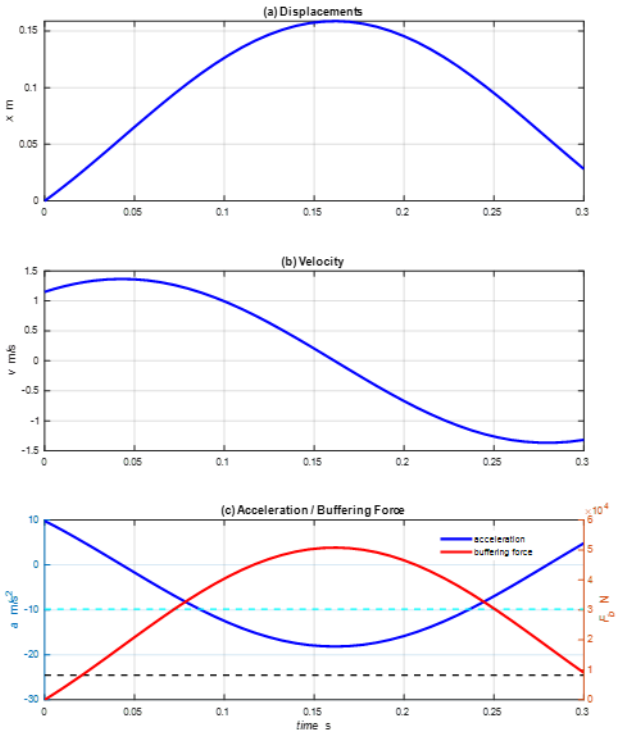


Figure 4 Linear accumulation buffer performance – car in free fall

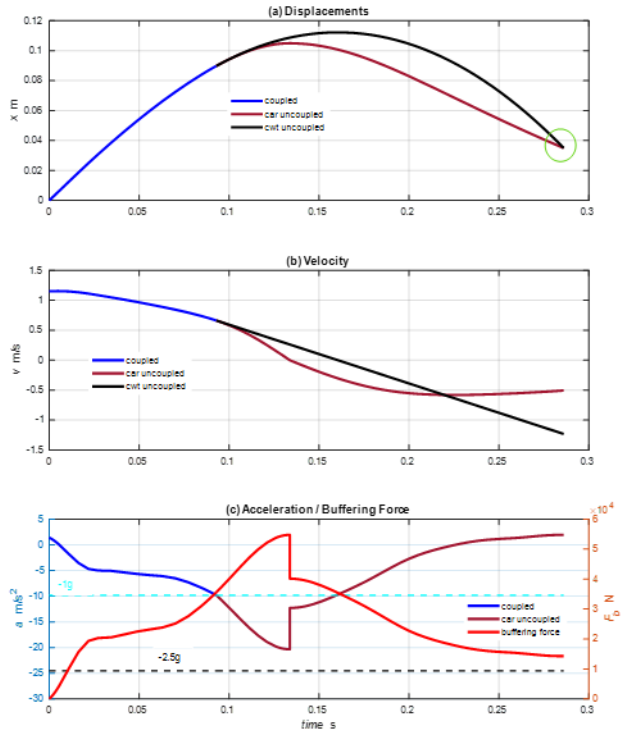


Figure 5 Non-linear accumulation buffer performance, intact suspension

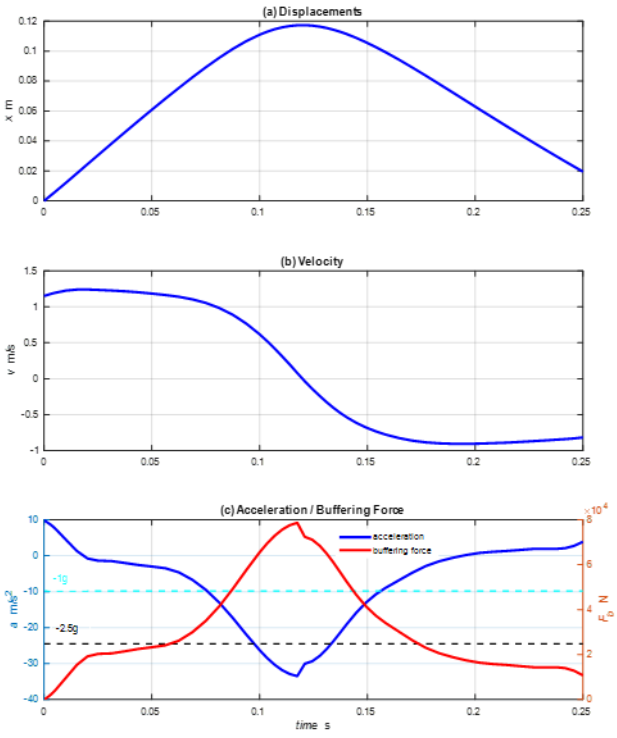


Figure 6 Non-linear accumulation buffer performance, car in free fall

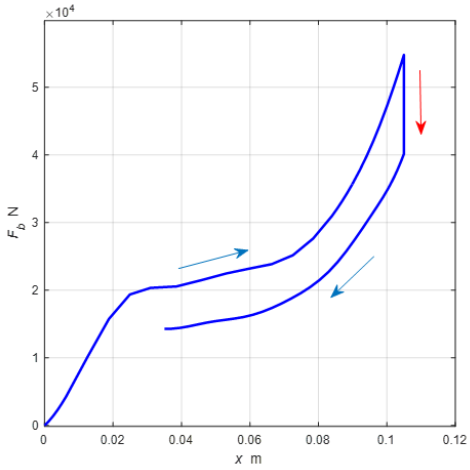


Figure 7 Non-linear buffer force vs stroke – intact suspension simulation

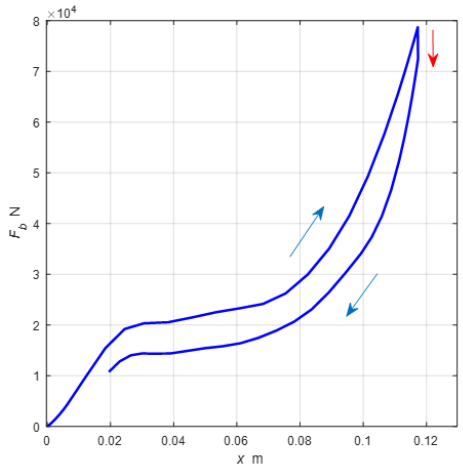


Figure 8 Non-linear buffer force vs stroke – car free fall simulation

3.2 Performance example of energy dissipation buffers

In this example, the rated speed of the lift is set to 2 m/s. A hydraulic buffer of rated speed 2.5 m/s and maximum stroke $s_{max} = 0.65$ m is used to illustrate the buffering event. The characteristic of effective orifice area versus stroke is given by Equation 27 [5].

$$A_o(x) = A_f + \sqrt{1 - \frac{x}{s_{\max}}}\left(A_{ini} - A_f\right) \tag{27}$$

In Equation 27, the initial cross-sectional area A_{ini} and final cross-sectional area A_f of the orifice are assumed as $A_{ini} = 3.0\times10^{-4}$ m^2 and $A_f = 0.05\times10^{-4}$ m^2, respectively. Figures 9 and 10 illustrate the time-dependent variation of displacement, velocity, deceleration, and buffering forces over the interval corresponding to the buffer stroke duration, for the cases of intact suspension and free fall,

respectively. The results are obtained through a numerical solution of Equation 24 for the intact suspension case, while Equation 4 and Equation 23 are applied to simulate the buffering event with the car in free fall. The coefficient of discharge $C_d = 0.7$ is used in the simulation tests. As pointed out above, the return spring accumulates only a small proportion of the energy during a buffering process. The spring constant value $k = 13.3$ kN/m is assumed in the simulation, which corresponds to about 15% of the total energy of the car to be dissipated during the buffering event. Over the time interval corresponding to the buffer stroke, the deceleration of the car with intact suspension varies from about 6.4 m/s^2 at the instant of impact to 1.2 m/s^2 at the end of the buffer stroke, respectively. Thus, with the decelerations maintained below 1g, the car and counterweight remain coupled via the suspension ropes over the buffer stroke. Theoretically, a hydraulic buffer can be designed to provide a constant rate of deceleration over the length of its stroke. Considering the results shown in Figure 10, the deceleration of the car in free fall remains quite uniform, varying slightly from about 4.2 m/s^2 to 3.3 m/s^2 over the buffer stroke.

4 CONCLUSION

Simplified models for predicting the dynamic behaviour of a lift system during overtravel under buffer-strike conditions have been presented and discussed in the paper. Although the models have certain limitations – notably the neglect of rope flexibility in simulations involving intact suspension – they demonstrate the dynamic behaviour of the lift during buffering events, both with intact suspension and when the car is in free fall. In general, cases with intact suspension exhibit lower acceleration levels and reduced buffering forces compared with free-fall conditions. In addition, energy-dissipating hydraulic buffers are designed to provide more controlled deceleration, making counterweight jump phenomena less likely to occur in events where suspension remains intact.

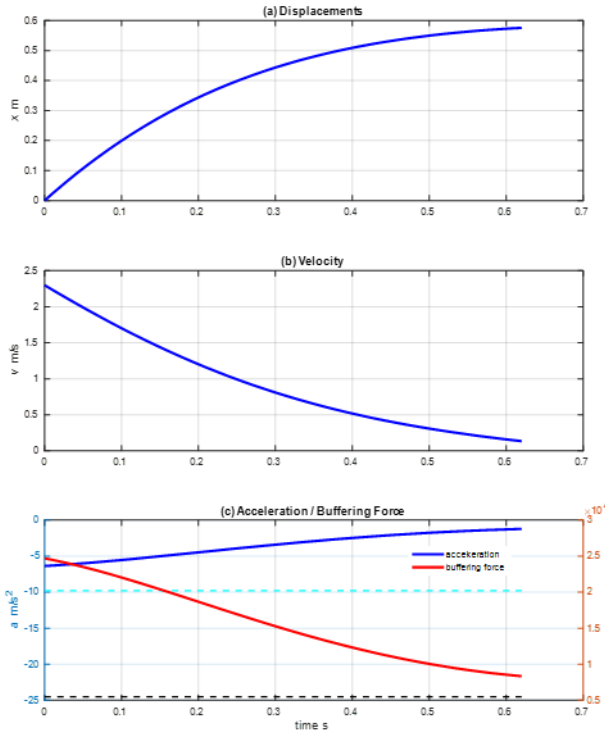


Figure 9 Energy dissipation buffer; displacements, velocity, deceleration and buffering force (intact suspension)

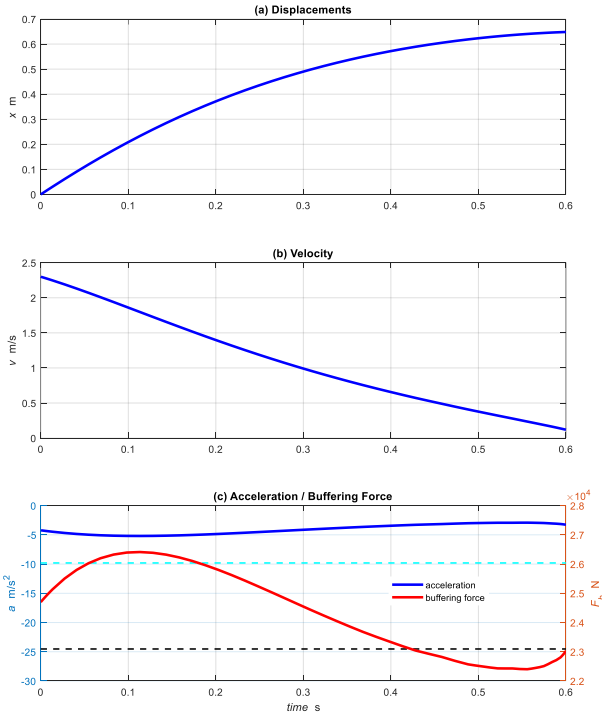


Figure 10 Energy dissipation buffer; displacements, velocity, deceleration and buffering force (free fall)

REFERENCES

[1] British Standards Institute, *Safety rules for the construction and installation of lifts — Lifts for the transport of persons and goods Part 20: Passenger and goods passenger lifts.* BS EN 81-20:2020. London: BSI.

[2] N. Mellor, "Non-linear energy accumulation buffers". *Proceedings of the 3rd Symposium on Lift and Escalator Technologies*. 26-27 September 2013, Northampton, UK.

[3] J.P. Andrew and S. Kaczmarczyk, *Systems Engineering of Elevators*. Elevator World, Mobile, AL (2011).

[4] British Standards Institution, *Safety rules for the construction and installation of lifts — Examinations and tests Part 50: Design rules, calculations, examinations and tests of lift components.* BS EN 81-50:2020. London: BSI.

[5] S. Vöth, Exploiting the Capacity of Industrial Hydraulic Buffers. In: *Proceedings of the 14th Symposium on Lift and Escalator Technologies*, Northampton, UK, 20 -21 September 2023.

[6] R. Li, G. Chen and P. Liang, "Modelling and finite element analysis of the hydraulic buffer in elevator systems". *Journal of Civil Engineering Research,* Vol. 7, No. 2, 63-66 (2017).

BIOGRAPHICAL DETAILS



Professor Stefan Kaczmarczyk's expertise is in applied mechanics/ dynamics and mathematical modelling, with applications to vertical transportation systems. He has over 45 years' research and consulting experience in these areas, and he taught mechanical engineering/engineering dynamics courses at all levels. Professor Kaczmarczyk is a Chartered Engineer, a Fellow of Higher Education Academy, elected Fellow of the Institution of Mechanical Engineers and Fellow of the Society of Vertical Transportation.